

Electronic distribution and second-harmonic generation at the metal-electrolyte interface

Wolfgang Schmickler*

Physics Department, Utah State University, Logan, Utah 84322

M. Urbakh

School of Chemistry, Tel Aviv University, Tel Aviv, 69978, Israel

(Received 23 December 1991; revised manuscript received 4 August 1992)

A model for second-harmonic generation at the metal-solution interface is presented in which the metal is modeled as jellium, and the solution is characterized by its optical dielectric constant. The coefficient a characterizing the nonlinear optical response perpendicular to the surface is calculated both for bare metal electrodes and for metals covered with an overlayer of a different metal. Generally, the presence of the solution reduces the absolute value of a , particularly for negatively charged surfaces, while a metal overlayer enhances it. Our calculations are compared with similar results for metal surfaces in the vacuum, and discussed with respect to experimental findings.

I. INTRODUCTION

In the past decade second-harmonic generation (SHG) has become a powerful tool for the investigation of the microscopic structure and dynamics of interfaces.¹⁻³ One of the main reasons for the interest in this nonlinear optical technique is its inherent surface sensitivity; SHG can provide information about the electronic and structural properties of atomically thin layers at surfaces and interfaces.

The application of SHG in electrochemistry is of particular importance since there are very few other methods which can probe the electronic structure of electrodes *in situ*. In contrast to surfaces in the vacuum, the electrochemical interface has an advantage in that the surface charge can be controlled by adjusting the applied external potential. This makes it possible to change the electron density distribution at the interface and the amount of adsorbed species, and to study the influence of these effects on the nonlinear optical response. By contrast, temperature is the only thermodynamic variable in the vacuum.

A large gap currently exists between theory and experiment on SHG in electrochemical systems. Numerous experimental studies have employed SHG as a tool for measuring the electronic, structural, and thermodynamic properties of components in the electrochemical double layer.^{1,3} The only microscopic calculation of the nonlinear optical response at the metal-electrolyte interface^{4,5} was done on the basis of an oversimplified model for the electronic density distribution at the surface. This model does not reproduce with reasonable accuracy the results of density-functional calculations^{6,7} for metal surfaces in the vacuum, and is limited to small surface charge densities. On the other hand recent density-

functional calculations⁶⁻¹⁰ of the nonlinear optical response for metals in the vacuum have enjoyed significant success. The dependence of the SHG signal on the angle of incidence, polarization, and frequency of the incident laser beam have been analyzed within the framework of the jellium model. Some of the theoretical predictions have been verified by quantitative measurements on aluminum surfaces. The results of the cited papers⁶⁻¹¹ clearly indicate that (i) the SHG response normal to the surface is quite sensitive to the electronic density profile at the surface, and (ii) a realistic description of the ground-state electron-density profile is necessary to explain experimental observations.

This paper reports on systematic density-functional calculations of the SHG response at a metal-electrolyte interface on the basis of realistic models for the electronic density profiles.^{12,13} The variation of the SHG signal with the electronic density n of the metal and the electrode charge density q have been studied. The effect of the adsorption of metallic overlayers on the SHG response is also considered. During the past few years this effect, which occurs primarily during the so-called underpotential deposition of metals, has been of special interest to experimentalists,^{3,14,15} but so far there is no theory for it.

In this work metal substrates and metal adsorbate layers are treated within the jellium model. This model neglects interband transitions, but provides a realistic description of the density distribution in the surface region. It describes the basic properties of simple metal surfaces quantitatively. The free-electron-like aspects of the conduction electrons of noble metals such as silver and copper should also be adequately represented by this model.

The theory presented below is intended to describe the SHG response at low frequencies. In this limit the normal component of the second-order polarization is nearly

independent of the frequency ω of the incident laser beam, and can be obtained from the nonlinear density induced by a static uniform electric field oriented perpendicular to the surface.^{8,9} We expect our results to be representative of the region $\omega/\omega_p < 0.1$ where ω_p is the bulk plasma frequency.

II. THE STRUCTURE OF THE SHG SIGNAL

Let us assume that p -polarized light of frequency ω is incident on a semi-infinite jellium. The intensity $I_{2\omega}$ of the SHG signal with p polarization may be expressed as follows:^{10,16}

$$\frac{I_{2\omega}}{I_\omega^2} = \frac{8\pi e^2}{m^2 \omega^2 c^3} \left| \frac{\epsilon_s(\omega)\epsilon_s(\Omega)\epsilon_m(\omega)[\epsilon_m(\omega) - \epsilon_s(\omega)]}{\epsilon_m(\Omega) + s(\Omega)} (P \cos^2\Psi + S \sin^2\Psi) \tan\theta \right|^2, \quad (1)$$

where

$$P = \frac{a(\omega) \frac{\epsilon_m(\Omega)\epsilon_s(\omega)}{\epsilon_m(\omega)} \sin^2\theta - b(\omega) \frac{2s(\omega)s(\Omega)}{\epsilon_m(\omega)\epsilon_s(\omega)} \cos^2\theta + \frac{1}{2}d(\omega)}{[\epsilon(\omega) + s(\omega)]^2},$$

$$S = \frac{d(\omega)}{2\epsilon_m(\omega)[\epsilon_m(\omega) + s(\omega)]^2}, \quad s(\omega) = \frac{[\epsilon_m(\omega) - \epsilon_s(\omega) \sin^2\theta]^{1/2}}{\cos\theta} \epsilon_s^{1/2}(\omega).$$

Here e , m , and c are the fundamental constants; $\Omega = 2\omega$; $\epsilon_m(\omega)$ and $\epsilon_s(\omega)$ are the bulk optical dielectric constants of the metal and the electrolyte, respectively. The polar angle of incidence with respect to the surface normal is denoted by θ ; Ψ is the angle of the polarization vector with respect to the plane of incidence ($\Psi = 0$ corresponds to p polarization, $\Psi = 90$ to s polarization). The amplitude $b(\omega)$ specifies the contribution to the signal caused by currents induced parallel to the surface and $d(\omega)$ is due to the magnetic dipole contribution from the bulk. In a semi-infinite free-electron system, the parameters d and b have the values $b = -1$, $d = 1$ and are independent of frequency and of the nature of the metal.^{16,17} The dimensionless function $a(\omega)$, on the other hand, characterizes the nonlinear response due to currents driven perpendicular to the surface, and depends sensitively on the electronic properties of the interfacial region. It is proportional to the integrated normal component of the second-harmonic surface polarization.^{6-10,17} This function can be expressed through the dipole moment of the nonlinear surface screening charge $\delta n_2(z, \omega)$ induced by a uniform electric field normal to the surface and oscillating with the frequency ω .⁸⁻¹⁰

$$a(\omega) = -4n_m \int_{-\infty}^{\infty} dz z \delta n_2(z, \omega) / q_\omega^2. \quad (2)$$

Here the coordinate z is normal to the surface, n_m is the bulk electronic density of the metal, and $q_\omega(t) = q_\omega \exp(i\omega t)$ is the surface charge density induced by an electromagnetic field at the interface.

In the low-frequency limit, when the conduction electrons of the metal follow the oscillations of the incident electromagnetic field instantaneously, the electronic density profile depends on $q_\omega(t)$ in the same manner as on the static charge density q . Then the second-harmonic screening surface charge $\delta n_2(z, \omega)$ can be written in the form

$$\frac{\delta n_2(z, \omega)}{q_\omega^2} = \frac{1}{2} \frac{\partial^2 n[z; q + q_\omega(t)]}{\partial q_\omega^2} \Big|_{q_\omega=0} = \frac{1}{2} \frac{\partial^2 n_0(z; q)}{\partial q^2} \quad (3)$$

with $n_0(z; q)$ being the ground-state electronic density for a given surface charge density q . When calculating the derivatives required by Eq. (3) we must keep in mind that at the metal-electrolyte interface the derivatives over the static charge dq and the oscillating charge dq_ω are equivalent only for electronic degrees of freedom. Indeed, the other degrees of freedom (vibrational and librational) can respond only to dq but they are too slow to react to dq_ω . Within the approximation adopted here the parameter $a(\omega)$ is independent of frequency and Eq. (3) reduces to⁴⁻⁷

$$a(\omega) = a = -2n_m \int_{-\infty}^{\infty} dz z \frac{\partial^2 n_0(z; q)}{\partial q^2}. \quad (4)$$

The ground-state density $n_0(z; q)$ can be obtained from a variational calculation assuming a particular form of the energy functional $E[n(z; q)]$ of jellium; from this the parameter a characterizing the nonlinear response perpendicular to the surface can be obtained. In the following we shall present such model calculations of a for the metal-solution interface; in particular we shall investigate its dependence on the electrode charge q and on the electronic characteristics of adsorbed monolayers.

III. THE SURFACE ELECTRONIC DENSITY PROFILE

For the calculation of the ground state electronic density we shall apply the trial function version of the variational procedure. In the case of bare metals in the vacuum or in contact with an electrolyte solution we shall use the two-parameter class of trial functions proposed in Ref. 12 which, in contrast to the functions commonly

used, accounts both for Friedel oscillations in the metal and for the Budd-Vannimenus theorem.¹⁸ This class of trial functions reproduces the results of the exact calculations by Lang and Kohn¹⁹ remarkably well, and seems particularly suited for the investigation of charged surfaces and such complicated systems as the electrochemical interface. The functions in question can be written as follows:¹²

$$n_0(z, q) = n_m \begin{cases} 1 - Ae^{\alpha z} \cos(\gamma z + \delta) & \text{for } z < 0 \\ Be^{-\beta z} & \text{for } z > 0. \end{cases} \quad (5)$$

Here the constant positive background charge, which represents the metal ions, occupies the half-space $z < 0$; the external medium (solution or vacuum) occupies the half-space $z > 0$, and in our model is characterized by its optical dielectric constant ϵ_∞ (for aqueous solutions we used the value $\epsilon_\infty = 1.88$). We chose the optical dielectric constant for the following reasons. (1) The incident laser beam typically has a frequency in or near the optical region, so that the optical dielectric constant must always be used in the calculation of δn_2 . (2) The penetration length $1/\beta$ of the electrons into the solution is of the order of 1, which is of the same order of magnitude as the correlation length of the electronic polarization of the solution, while the correlation lengths for the vibrational and librational polarization are larger, of the order of the diameter of the solvent molecule (~ 3). So, to a first approximation, it is reasonable to use the optical dielectric constant both for the calculation of $n_0(z, q)$ and its variations. Nevertheless, second-order effects due to the interaction of the static electronic distribution with the other polarization modes may exist. Several groups have used a somewhat higher "effective" dielectric constant in the range $\epsilon = 4-6$ for this reason; however, this value must not be used for the calculation of δn_2 since this varies with a frequency in the optical region.

The trial functions in Eq. (5) contain six undetermined parameters: A , B , α , β , γ , and δ ; they must satisfy the following relations: (1) continuity of $n(z, \omega)$ and (2) its first derivative, (3) charge balance, and (4) the half-moment condition (Budd-Vannimenus theorem),¹⁸ which has been modified to account for the presence of a dielectric medium in the half-space $z > 0$. The remaining two free parameters are determined by minimizing the functional of the surface energy. For negative charge densities on the metal the energies of the one-electron states do not have a lower bound, since the energies of states localized in the vacuum outside the metal can be arbitrarily low. Minimization is then performed within the subspace of states pertaining to the metal, which decay in the barrier region in $z > 0$. We have used the Wigner approximation for the exchange and correlation energy as given in the paper by Smith;²⁰ for the kinetic energy we have employed the gradient expansion keeping terms up to second order. The latter term was taken in the form proposed by Ma and Sahni.²¹

The true solution for the electronic density of jellium exhibits Friedel oscillations in the surface region, which decay as $1/|z|$ and have a wave number of $2k_F$. The parametrization (5) does not have this asymptotic behavior.

However, as it was shown in Ref. 12, variational solutions obtained with this family do have the correct amplitude and frequency of oscillation in the important interfacial region, and they give very good values for the work function and the position of the effective image plane. Use of the Budd-Vannimenus theorem ensures that the contributions of the region $z < 0$, which encompasses the Friedel oscillations, to the work function, the image plane position, and to the second-harmonic response a , are calculated exactly.

Calculations for the adsorbate covered metals were done with the three-parameter family of trial functions used previously in Ref. 13. Following the work of Lang,²² we represent the adsorbate layer as a jellium slab of thickness d and a background charge density n_{ad} placed on top of the jellium substrate. In the adopted model the positive background charge is

$$n_+(z) = n_m \theta(-z) + n_{ad} \theta(z) \theta(d-z), \quad (6)$$

where $\theta(z)$ denotes the Heaviside function. For the problem at hand, we have taken electron-density trial functions of the form

$$n(z) = \begin{cases} n_m [1 - Ae^{\alpha z}] & \text{for } z < 0 \\ n_m Be^{-\beta z} + n_{ad} [1 - Ce^{\gamma(z-d)}] & \text{for } 0 < z < d \\ n_m Be^{-\beta z} + n_{ad} De^{-\delta(z-d)} & \text{for } d < z. \end{cases} \quad (7)$$

Continuity of $n(z)$, its first derivative, and the condition of charge balance reduce the number of unknown parameters A , B , C , D , α , β , γ , and δ to three independent ones. These free parameters are determined by minimization of the same surface energy functional which we used for the bare metal surface. This simple family of trial functions has been successfully employed in a model for the adsorption of a metal overlayer (underpotential deposition) on the surface of a metal substrate in electrochemical systems.¹³

IV. RESULTS AND DISCUSSION

A. The electrochemical interface without a metallic overlayer

We have performed model calculations of the nonlinear response both for uncharged and charged jellium surfaces at different values of the bulk electronic density n_m of the metal. Figure 1 shows the dependence of the parameter a on n_m or, equivalently, the Wigner-Seitz radius $r_s = (4\pi n_m / 3)^{-1/3}$, for uncharged surfaces in contact with an aqueous electrolyte and in the vacuum. For comparison the results of the local-density approximation (LDA) calculations of Weber and Liebsch⁶ (WL) carried out for metals in the vacuum are also presented. Our vacuum curve and that of WL agree very well with the exception of the point at $r_s = 2$ a.u. To verify the correctness of our approach at large values of the electronic density we have calculated the parameter a also for a jellium model using the exact expression for the kinetic energy and the expansion technique proposed by Mola and Vicente.²² For $n_m = 26.8 \times 10^{-3}$ (Al), using 48 basis functions, we obtained $-a = 24$. This value lies between that of WL and the result of our variational calculation. It should be noted that calculations with the two-parameter

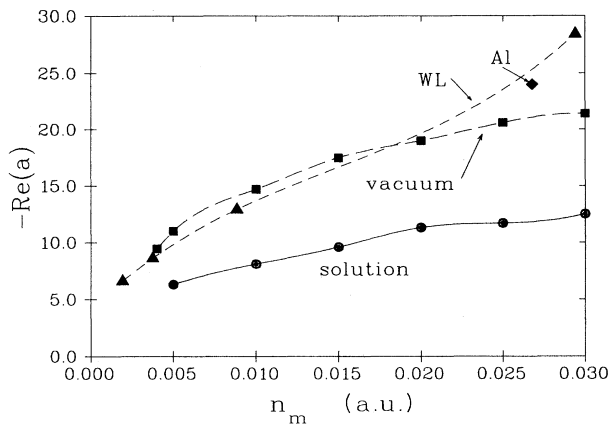


FIG. 1. SHG parameter a on bare metals as a function of the electronic density n_m .

trial function (which simulate the asymmetry of surface electronic profile) agree much better with the LDA results than calculations using one-parameter symmetric trial functions.^{4,5} For the metal-electrolyte interface the absolute value of the parameter a is smaller than for the vacuum case due to the screening of the electric field in the solution ($\epsilon_\infty = 1.88$).

Figure 2 demonstrates the charge dependence of the second-order response $a(q)$ for Al (note: 1.8×10^{-4} a.u. = $1 \mu\text{C}/\text{cm}^2$). We see that in the presence of the solution this dependence is weaker than in the vacuum; the absolute value of a is also smaller for reasons discussed above. This difference disappears in the range of large positive charges since the overlap between the electronic tail and the medium becomes smaller. For positively charged surfaces, the electronic distribution is pushed into the metal and becomes stiffer. This leads to an overall decrease of the second-harmonic polarizability. These results illustrate the remarkable sensitivity of the normal component of nonlinear surface polarization to the state of the surface.

Figures 3 and 4 give the dependence of the nonlinear

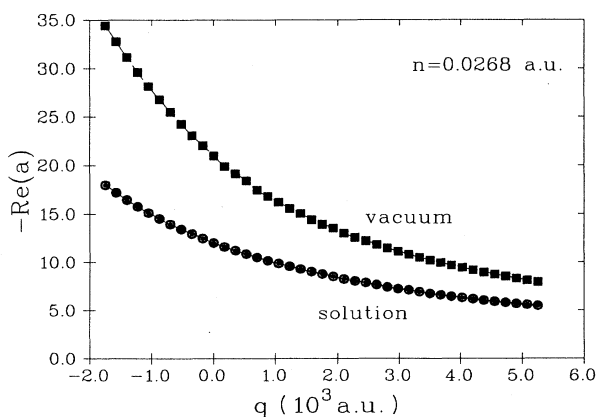


FIG. 2. SHG parameter a for aluminum as a function of the charge density q .

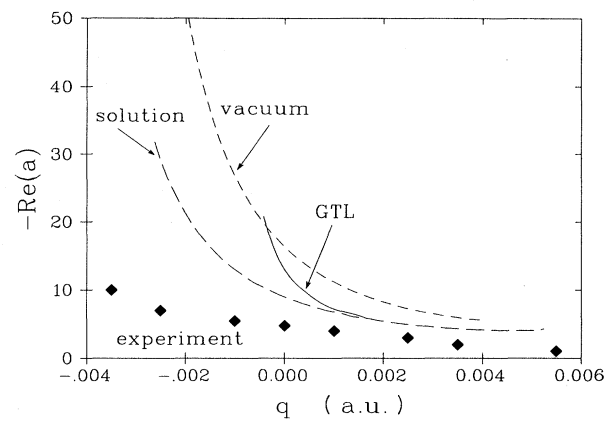


FIG. 3. SHG parameter a for silver as a function of the charge density q . The curve labeled GTL was obtained from Ref. 24 as described in the text. Experimental points are also from Ref. 24.

optical coefficient a on the surface charge q for Ag either in the vacuum or in contact with an electrolyte. Our treatment of the electronic properties of Ag is based on the paper by Amokrane and Badiali,²³ according to which we have included 1.5 electrons per silver atom into the free-electron density ($n_m = 0.013$ a.u.). The points are the measured values²⁴ of $-\text{Re}a(\omega)$ at $\hbar\omega = 1.17$ eV. Since in aqueous solutions silver is oxidized at higher positive potentials,²⁵ we have not considered experimental points in this region. The imaginary part of $a(\omega)$ is rather small at this frequency.²⁴ The solution curve is closer to the experimental one than the vacuum curve, but still $a(q)$ is too large at negative charges. For comparison we also show the theoretical curve of Ref. 24 (labeled GTL) for silver based on an exact calculation for jellium with a density of 8.6×10^{-3} a.u. (one free electron per silver

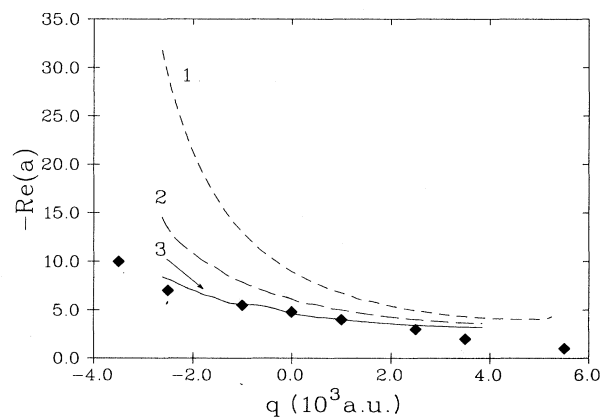


FIG. 4. SHG on silver in contact with an aqueous solution (1) without an external barrier, (2) with a barrier of slope $V_0 = 0.5$ eV/Å, and (3) with a barrier of slope $V_0 = 1.0$ eV/Å. The diamond-shaped symbols indicate the experimental points from Ref. 24.

atom) in the vacuum. However, the authors of that paper scaled the results of their calculation by multiplying all charges by a factor of 6 to account for the presence of the solution. Since we think that this procedure is unjustified we have reconstructed their original curve. The GTL curve and our vacuum curve differ because of the different electronic densities employed in the calculations. Using the model of Amokrane and Badiali for silver and accounting for the presence of the solution in the jellium calculations leads to a much better agreement with experimental data.

The discrepancy between our calculated curve and the experimental data at negative charges may be due to the repulsion that the electrons experience from the water molecules, an effect which must surely be present but which is not included in our model. To mimic this effect we have performed calculations with an external barrier of the form $V(z) = V_0 z \theta(z)$ on the solution side. This introduces an extra term into the energy functional, and also modifies the Budd-Vannimenus sum rule; details are given in Ref. 26. Such a barrier is most effective at negative charges, where it pushes the electronic tail back into the metal and reduces its linear and nonlinear polarizability, and brings the calculated curve closer to the experimental values. Curves 2 and 3 in Fig. 4 were obtained for values of $V_0 = 0.5$ and 1 eV/\AA , respectively. The latter curve is seen to fit the experimental data quite well. However, it should be mentioned that there are other possible reasons for the reduction of the calculated values of $a(q)$ at negative charges. Whereas the jellium model gives quantitative agreement with SHG measurements on Al,¹¹ in the case of Ag it seems to overestimate the surface nonlinear polarization. Electronic structure calculations for Ag(100) using the surface embedding method²⁷ give a value for $a(0)$ at zero charge which is about one-third the jellium value as a result of band-structure effects. Calculations for jellium with pseudopotentials give a similar reduction of the nonlinear polarizability compared with the simple jellium version.²⁸ Furthermore, an additional reduction of $-a(q)$ at negative charges could be caused by the orientation of water molecules at the surface, an effect not included in our model.

Figure 5 shows the results of calculations for the total SHG signal (p -in, p -out configuration) at a silver-electrolyte interface as a function of the electrode charge q for various angles of incidence θ . It is seen that the position of the minimum for each curve depends strongly on the angle of incidence. This effect was observed in a recent report by Guyot-Sionnest and Tadjeddine,²⁹ and was attributed to the interference of charge-dependence and charge-independent sources of the nonlinear polarization, and the angular dependence of the Fresnel coefficients appearing in Eq. (1). For $\theta = 45^\circ$ the minimum is right at the point of zero charge (PZC), but this is a purely accidental phenomenon for silver. A parabolic behavior of the SHG response near the PZC was observed in a number of experimental papers^{1,3} where an angle of incidence close to 45° was used. Corn *et al.*³⁰ proposed a phenomenological model for the observed behavior from these studies. Their model predicts that the SHG signal should scale quadratically with the surface charge density.

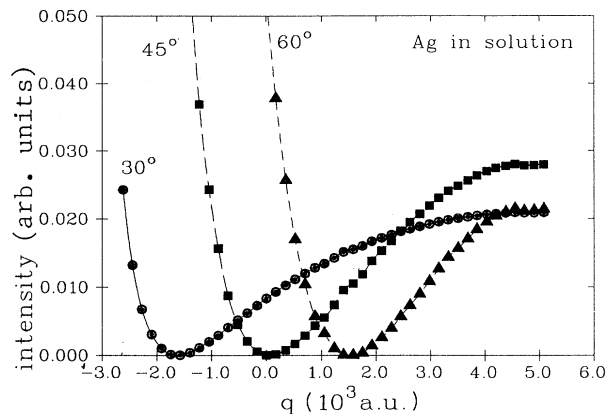


FIG. 5. SHG response at various angles of incidence for Ag in an aqueous solution.

There were also attempts³¹ to use the parabolic behavior of SHG near the PZC to determine the latter. However, our calculations show that this behavior is not general and depends on the nature of the metal and on the angle of incidence. It should be also mentioned that surface roughness affects the experimentally observed charge dependence of SHG.^{1,3}

B. The electrochemical interface with metallic overlayers

Numerous experimental studies^{1-3,14,15} show that SHG is very sensitive to the presence of even submonolayers of metals deposited or absorbed on the surface of a metal substrate. To describe the influence of metallic overlayers on the SHG response from an electrochemical interface we shall apply the model discussed in Sec. III. The density-functional (LDA) treatment of a similar model^{6,10} was successfully used for the explanation of SHG by alkali-metal overlayers in the vacuum.

Figure 6 demonstrates the effect of metal monolayers of various densities n_{ad} adsorbed on Al ($n_m = 0.0268 \text{ a.u.}$) in contact with an electrolyte or in the vacuum. The nonlinear parameter $-a$ is much larger in the presence of a metal overlayer than for bare metals with the same electron density (see Fig. 1), and increases with increasing difference $n_m - n_{ad}$ between the densities of the substrate and adsorbate. These effects can be explained by the following arguments.¹⁰ The quantity n_m in the definition of $a(q)$, Eqs. (2) and (4), refers to the average electron density deep inside the substrate, which determines, via the bulk plasma frequency, the asymptotic behavior of the electric field in the interior. Thus, for the metal overlayers shown in Fig. 6, this quantity is enhanced by the ratio $n_m(\text{Al})/n_{ad}$ compared to bulk metals with an electronic density $n_m = n_{ad}$. The values of the parameter $a(q)$ for metal overlayers are also enhanced by about these ratios as compared to the bare surfaces of the same metals (compare Figs. 1 and 6):

$$a_{ad}(n_{ad}/n_m) \simeq (n_m/n_{ad})a(n_{ad}), \quad (8)$$

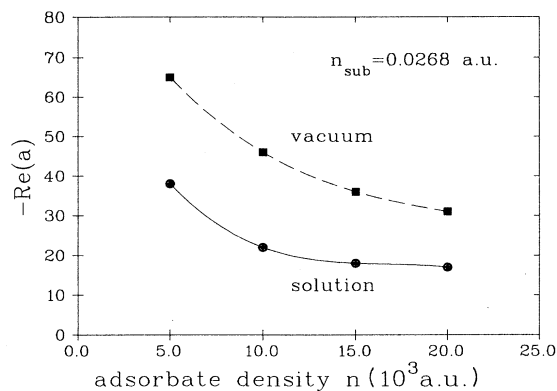


FIG. 6. SHG parameter a for a metal overlayer adsorbed on a high-density metal (Al) in the absence of surface charges.

where $a(n_{ad})$ and $a_{ad}(n_{ad}/n_m)$ are the nonlinear parameters for bare metals with electronic density n_{ad} and for the metal overlayer with density n_{ad} on the substrate with density n_m . For bare metal surfaces the nonlinear parameter $-a$ decreases slowly (slower than n_m) with decreasing electronic density n_m (see Fig. 1). This effect and Eq. (8) lead to the increasing of the quantity $-a$ with decreasing adsorbate density n_{ad} as shown in Fig. 6. Obviously such behavior cannot go on indefinitely: for $n_{ad}=0$ the enhancement must disappear.

Figure 7 gives the dependence of the parameter $-a$ on the thickness of a metal overlayer on Al. We modeled the overlayer by using a slab with a constant density n_{ad} , and by allowing the thickness to vary from zero to any value. One can also model the overlayer using a homogeneous positively charged slab of thickness d whose density n increases from zero to that of the bulk metal as the coverage is increased from zero to one monolayer. The second overlayer then has the same thickness d and its density also varies from zero to the bulk value of the overlayer metal. The two models can yield different behavior during the deposition of the second layer.⁷ This disagreement between the two models is a consequence of

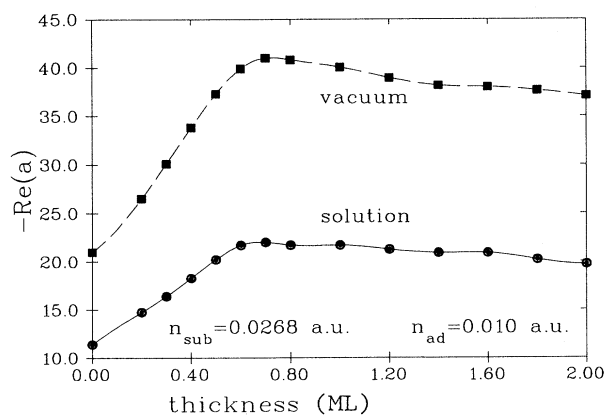


FIG. 7. SHG parameter a as a function of the thickness of the adsorbate layer for an uncharged surface.

an oversimplified simulation of an atomic overlayer by a thin jellium slab. But results for coverages between zero and one monolayer usually show qualitatively the same behavior in both models.

For overlayers with an electronic density of $n_{ad}=0.010$ a.u. in the vacuum or in an aqueous solution the parameter $-a$ increases at small coverages and has a maximum at $\theta=0.7$ in the former case and $\theta=0.6$ in the latter; $-a$ becomes smaller if the coverage is increased further. The physical reason for this variation is that the electronic density becomes more polarizable as it is pulled out of the metal in the presence of the overlayer with an electronic density $n_{ad} < n_m$. Within the jellium slab model partial coverages correspond to thinner adsorbed jellium layers. Thus (see also Fig. 6), the stronger enhancements of nonlinear response, $-a$ could be obtained at coverages less than a full monolayer. Similar conclusions were obtained in Refs. 7 and 10 on the basis of LDA calculations of alkali-metal overlayers in the vacuum. For the electrochemical interface the maximum in the $-a$ vs q curve is not so pronounced as in the vacuum case.

Figure 8 shows the intensities of the reflected SHG signal (p -in, p -out configuration) in the vacuum and at metal-electrolyte interfaces as functions of the metal adsorbate coverage. Both curves demonstrate a drastic coverage-dependent enhancement of the second-harmonic intensity due to the formation of the overlayers with maxima at coverages below that of a single full monolayer. Again at the metal-electrolyte interface the effect is not so pronounced as in the vacuum case. Qualitatively similar enhancements of the SHG signal by an adsorbed metallic overlayer have been observed experimentally both in the vacuum and at the electrochemical interface.^{3,14,15,32} Our calculations show that, even without considering optical transitions in the interfacial region, changes in the electronic density profile induced by metal overlayers can lead to a dramatic enhancement of the parameter a characterizing the nonlinear response perpendicular to the metal surface. The effect of adsorption on this parameter is stronger than that of double-

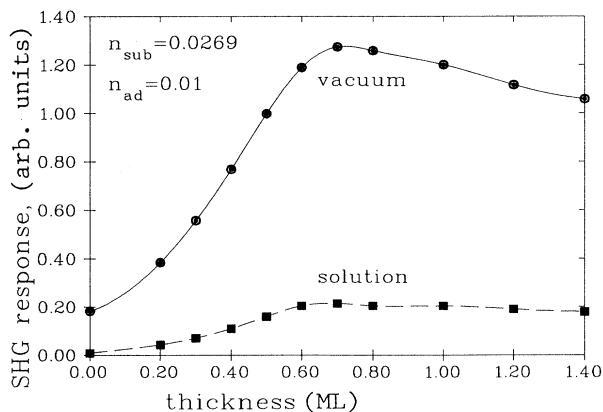


FIG. 8. SHG intensity as a function of the thickness of the adsorbate layer for an angle of incidence of 45° in the p -in p -out configuration for an uncharged surface.

layer charging. We hope that this effect can be used for *in situ* studies of the electronic properties of adsorbates. However, it should be noted that for low-density metal adsorbates (such as alkali-metal atoms) the frequency dependence of the parameter a neglected in our static theory can be important.

V. CONCLUSION

The work presented above is one of the first theoretical investigations into second-harmonic generation at the electrochemical interface. We have used much better representations for the electronic density profile than pre-

vious studies^{4,5} and, with the exception of the two curves in Fig. 5 showing the effect of an external barrier, our calculations contain no adjustable or arbitrary parameters. Our model suggests a noticeable effect of the solution on the SHG signal, in particular a significant reduction of the absolute value of the parameter a characterizing the nonlinear response perpendicular to the surface; this effect is more marked at negative charge densities, where the electrons penetrate more deeply into the solutions, and disappears at high positive charges. Our results explain at least qualitatively a number of effects observed experimentally; in particular they illustrate the sensitivity of the SHG signal to the electronic properties of the electrode surface.

*Permanent address: Abteilung Elektrochemie, Universität Ulm, D-7900 Ulm, Germany.

- ¹G. L. Richmond, I. M. Robinson, and V. L. Shannon, *Prog. Surf. Sci.* **28**, 1 (1988); *Electrochim. Acta* **34**, 1639 (1989).
- ²Y. R. Shen, *Nature* **337**, 519 (1989).
- ³G. L. Richmond, in *Electroanalytical Chemistry*, edited by A. J. Bard (Dekker, New York, 1991), Vol. 17, p. 87.
- ⁴P. G. Dzhavakhidze, A. A. Kornyshev, A. Liebsch, and M. I. Urbakh, *Electrochim. Acta* **36**, 1835 (1991).
- ⁵P. G. Dzhavakhidze, A. A. Kornyshev, A. Liebsch, and M. I. Urbakh, *Phys. Rev. B* **45**, 9339 (1992).
- ⁶M. Weber and A. Liebsch, *Phys. Rev. B* **35**, 7411 (1987).
- ⁷M. Weber and A. Liebsch, *Phys. Rev. B* **36**, 6411 (1987).
- ⁸A. Liebsch, *Phys. Rev. Lett.* **61**, 1233 (1988).
- ⁹A. Liebsch and W. L. Schaich, *Phys. Rev. B* **40**, 5401 (1989).
- ¹⁰A. Liebsch, *Phys. Rev. B* **40**, 3421 (1989).
- ¹¹M. Murphy, M. Yeganeh, K. J. Song, and E. W. Plummer, *Phys. Rev. Lett.* **63**, 318 (1989).
- ¹²W. Schmickler and D. Henderson, *Phys. Rev. B* **30**, 3081 (1984).
- ¹³E. Leiva and W. Schmickler, *Chem. Phys. Lett.* **160**, 75 (1989).
- ¹⁴T. E. Furtak, J. Miragliotta, and G. M. Korenowski, *Phys. Rev. B* **35**, 2569 (1987).
- ¹⁵J. M. Robinson and G. L. Richmond, *Chem. Phys.* **141**, 175 (1990).
- ¹⁶J. Rudnick and E. A. Stern, *Phys. Rev. B* **4**, 4274 (1971).
- ¹⁷M. Corvi and W. L. Schaich, *Phys. Rev. B* **33**, 3688 (1986).
- ¹⁸H. F. Budd and J. Vannimenus, *Phys. Rev. Lett.* **31**, 1218 (1973).
- ¹⁹N. D. Lang and W. Kohn, *Phys. Rev. B* **1**, 4555 (1970); **3**, 1215 (1971); **7**, 3541 (1973).
- ²⁰J. R. Smith, *Phys. Rev.* **181**, 522 (1969).
- ²¹C. Q. Ma and V. Sahni, *Phys. Rev. B* **19**, 1290 (1979).
- ²²X. Mola and X. Vicente, *J. Chem. Phys.* **84**, 2876 (1986).
- ²³S. Amokrane and J.-P. Badiali, *Electrochim. Acta* **34**, 39 (1989); *J. Electroanal. Chem.* **266**, 21 (1989).
- ²⁴P. Guyot-Sionnest, A. Tadjeddine, and A. Liebsch, *Phys. Rev. Lett.* **64**, 1678 (1990).
- ²⁵A. Hamelin, T. Vitanov, E. Sebastianov, and A. Popov, *J. Electroanal. Chem.* **145**, 225 (1983).
- ²⁶W. Schmickler and D. Henderson, *J. Chem. Phys.* **85**, 1650 (1986).
- ²⁷G. C. Aers and J. E. Inglesfield, *Surf. Sci.* **217**, 367 (1989).
- ²⁸E. Leiva and W. Schmickler (unpublished).
- ²⁹P. Guyot-Sionnest and A. Tadjeddine, *J. Phys. Chem.* **92**, 1 (1990).
- ³⁰R. M. Corn, M. Romagnoli, M. D. Levenson, and M. R. Philippot, *J. Chem. Phys.* **81**, 4127 (1984).
- ³¹O. A. Aktsipetrov, V. Ya. Bertenev, and E. D. Mishina, *Elektrokhimiya* **20**, 477 (1984).
- ³²K. J. Song, D. Heskett, H. L. Dai, A. Liebsch, and E. W. Plummer, *Phys. Rev. Lett.* **61**, 1380 (1989).